Biochimica et Biophysica Acta 1780 (2008) 983–988

Contents lists available at ScienceDirect

Biochimica et Biophysica Acta

journal homepage: www.elsevier.com/locate/bbagen

Biophysical characterization of the recombinant merozoite surface protein-3 of *Plasmodium vivax*

Maria Carolina S. Jimenez [a], Carlos Henrique I. Ramos [b,c], João Alexandre R.G. Barbosa [b], Mary R. Galinski [d,e], John W. Barnwell [f], Mauricio M. Rodrigues [g], Irene S. Soares [a,*]

[a] *Departamento de Análises Clínicas e Toxicológicas, Faculdade de Ciências Farmacêuticas, Universidade de São Paulo, Av. Prof. Lineu Prestes, 580, Cidade Universitária, São Paulo, SP, 05508-900, Brazil*
[b] *Center for Structural Molecular Biology (CeBiME), Brazilian Synchrotron Light Laboratory, C.P. 6192, Campinas, SP, 13084-971, Brazil*
[c] *Instituto de Química UNICAMP. C.P. 6154 Campinas, SP, 13084-862, Brazil*
[d] *Emory Vaccine Center and Yerkes National Primate Research Center, Emory University, 954 Gatewood Road, Atlanta, GA 30329, USA*
[e] *Department of Medicine, Division of Infectious Diseases, Emory University, 954 Gatewood Road, Atlanta, GA 30329, USA*
[f] *Malaria Branch, Division of Parasitic Diseases, Centers for Disease Control and Prevention, 4770 Buford Highway, Chamblee, GA 30341, USA*
[g] *CINTERGEN, Departamento de Microbiologia, Imunologia e Parasitologia, Universidade Federal de São Paulo-Escola Paulista de Medicina, Rua Botucatu 862, 6th floor, São Paulo, SP, 04023-062, Brazil*

ARTICLE INFO

Article history:
Received 18 January 2008
Received in revised form 30 March 2008
Accepted 31 March 2008
Available online 7 April 2008

Keywords:
Malaria
Plasmodium vivax
Merozoite surface protein-3

ABSTRACT

Plasmodium vivax Merozoite Surface Protein-3α and 3β are members of a family of related merozoite surface proteins that contain a central alanine-rich domain with heptad repeats that is predicted to form α-helical secondary and coiled-coil tertiary structures. Seven recombinant proteins representing different regions of MSP-3α and MSP-3β of *P. vivax* were generated to investigate their structure. Circular dichroism spectra analysis revealed that some proteins are folded with a high degree of α-helices as secondary structure, whereas other products contain a high content of random coil. Using size exclusion chromatography, we found that the two smaller fragments of the MSP-3α, named CC4 and CC5, predicted to form coiled-coil (CC) structures, eluted at volumes corresponding to molecular weights larger than their monomeric masses. This result suggests that both proteins are oligomeric molecules. Analytical ultracentrifugation experiments showed that the CC5 oligomers are elongated molecules. Together, these data may help to understand important aspects of *P. vivax* biology.

1. Introduction

Malaria represents a major public health problem in many developing countries. There are an estimated 300 million to 500 million cases of malaria occurring each year throughout the world. Despite its high prevalence, *Plasmodium vivax* malaria is among today's neglected diseases [1] and [2]. In Brazil, *P. vivax* was responsible for approximately 73% of the 540,000 cases of malaria reported in 2006 [Secretaria de Vigilância em Saúde, Ministério da Saúde -http://www.saude.gov.br]. The strategies in use for malaria control, based on drugs and insecticides, have not succeeded in eliminating the disease so far. Along with these control measures, the development of an effective vaccine is considered an important priority [reviewed in [3]].

The asexual blood-stage parasites are responsible for the pathology and clinical manifestations of malaria. Therefore, a vaccine against these stages would greatly help to reduce morbidity and mortality related to this disease. Attempts have been made to identify and characterize asexual stage antigens that may induce a protective immune response against malaria. Several *P. vivax* merozoite-specific proteins have been described in the past 10 to 20 years; prior to the sequencing of the *P. vivax* genome, which has been in progress. These include the *P. vivax* Duffy Binding Protein (PvDBP) [4] and [5], Merozoite Surface Protein-1 (PvMSP-1) [6], Reticulocyte Binding Proteins-1 and -2 (PvRBP-1 and PvRBP-2) [7], Apical Membrane Antigen-1 (PvAMA-1) [8], PvMSP-3α, -3β, and -3γ, [9] and [10] and PvMSP-9 [11].

P. vivax MSP-3 proteins share structural similarity to *Plasmodium falciparum* MSP-3 (PfMSP-3). All of these proteins contain a central alanine-rich domain that is predicted to form α-helical secondary and coiled-coil tertiary structures with heptad repeats. These proteins do not have a hydrophobic region that could anchor them to the surface of the merozoite [9] and [10]. Rather, they are predicted to associate with other surface anchored proteins.

MSP-3α is highly polymorphic [12], and it has therefore been adopted as a molecular epidemiological marker in *P. vivax* population studies [13–18] and [19]. However, this polymorphism is restricted to the N-terminal half of the predicted coiled-coil domain, which can even be absent in some alleles, while the C-terminal portion is highly conserved [12]. On the other hand, analysis of the polymorphism of the MSP-3β from *P. vivax* isolates revealed a high degree of diversity, mostly throughout the alanine-rich central region [20]. Sequence block insertions and/or deletions and numerous single nucleotide polymorphisms were observed. However, this

* Corresponding author. Fax: +55 11 3813 2197.
E-mail address: isoares@usp.br (I.S. Soares).

0304-4165/$ – see front matter © 2008 Elsevier B.V. All rights reserved.
doi:10.1016/j.bbagen.2008.03.016

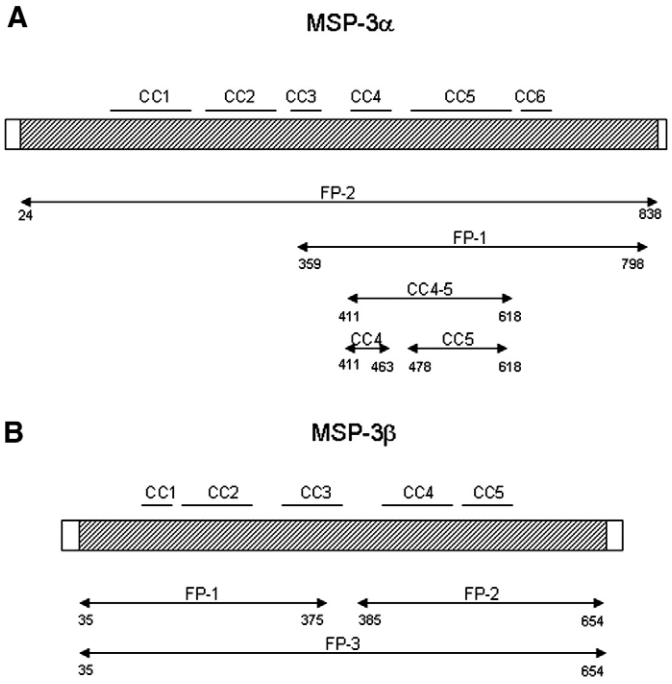

Fig. 1. Schematic representation of *P. vivax* MSP-3α (accession number AF093584) and MSP-3β (accession number AF099662). The shaded box represents the expressed full-length proteins MSP-3α and MSP-3β. The lines above each box represent the predicted coiled-coil (CC) tertiary structure region and the arrows below show the different his-tag fusion proteins (FP) based on MSP-3 produced for these experiments.

high level of sequence diversity does not impair the ability of each variant to form coiled-coil tertiary structures. Certain physical properties of the encoded proteins are maintained suggesting that MSP-3β cannot vary beyond specific functional constraints [20].

Structural studies of *Plasmodium* surface proteins can facilitate the understanding of their biological function and immunological properties [21]. The structural information available for MSP-3 of *Plasmodium* and/or its interaction with host or parasite proteins is limited at present. A single study on the structure and interactions between different regions of *P. falciparum* MSP-3 (PfMSP-3) has been published [22]. The recombinant full length of PfMSP-3 contains a large amount of -helix and random coil secondary structure and can form highly elongated dimers and tetramers via its C-terminus, which contains a small predicted coiled-coil region [22]. There is no data on the interactions of MSP-3 with other merozoite proteins. However, the interaction partners between different merozoite surface proteins (MSP-1, MSP-6, and MSP-7) of *P. falciparum* have been recently studied *in vitro* [23]. These proteins form a large multiprotein complex on the merozoite surface, composed of proteolytically processed, noncovalently associated products. The PfMSP-6 is related to PfMSP-3 [24] and the C-terminal region is not only crucial for the tetramerization of the protein but also for its interaction with MSP-1 [23]. During invasion of erythrocytes, this complex is shed from the surface and only a small glycosylphosphatidylinositol (GPI)-anchored portion originating from MSP-1 ($MSP1_{19}$) is carried into the invaded red cells [25].

In the present study, we have carried out the first assessment of biophysical characterization of recombinant proteins representing *P. vivax* MSP-3α and MSP-3β with the overarching aim to contribute knowledge relevant for the *P. vivax* biology. Initially, four recombinant proteins representing different regions of MSP-3α and MSP-3β of *P. vivax* were generated to characterize their structure. To investigate possible interaction between the regions that are predicted to form coiled-coil tertiary structures, we produced three other shorter recombinant proteins containing subsets of the predicted domains of the C-terminal region of MSP3-α.

2. Materials and methods

2.1. Generation of recombinant plasmid containing the P. vivax msp3α gene

The nucleotide sequences corresponding to the C-terminal region and almost full-length protein of *P. vivax* MSP-3α were obtained from the plasmids pGEX-1λT/FP-1 (aa 359–798) or pGEX-2T/FP-2 (aa 24–838) by enzymatic restriction with EcoRI or BamHI, respectively [3]. The inserts were purified and cloned into EcoRI-digested pHISa (FP-1) or BamHI-digested pHISb (FP-2). The pHIS plasmids used as bacterial expression vectors were kindly provided by Dr. P. Sheffield, University of Virginia [26]. After transformation in competent *Escherichia coli* DH5α, the colonies that contained the *msp3α* gene were selected by restriction analysis.

In addition, we generated other constructs corresponding to the C-terminus of MSP3α, which represent three areas (CC4 to CC5) that are predicted to form a coiled-coil tertiary structure as previously suggested by software analyses [9]. These recombinant plasmids were generated from pET28a vector (Novagen) encoding proteins CC4-5 (aa 411–618), CC4 (aa 411–463), and CC5 (aa 478–618) in fusion with a hexa-histidine tag (Fig. 1). The recombinant CC4 and CC5 contains eight and twenty heptads repeats, respectively. The three expression constructs were created by PCR amplification from the plasmid pGEX-2T/FP-2 and the following oligonucleotide primers: CC4-5 (forward: 5′-CAA GCT TGC AAA GCA TCG ATC GAA ACG ACG-3′; reverse: 5′-TGC TCG AGT TTA TGC CCC TAC TTT TGC TGC-3′); CC4 (forward: 5′-CAA GCT TGC AAA GCA TCG ATC GAA ACG ACG-3′; reverse: 5′-TGC TCG AGT TTA GTG GGT CTT TGC CTC TTC-3′); and CC5 (forward: 5′-CAA GCT TGC TCA GAT GAA GCA CAG CAA GAA-3′; reverse: 5′-TGC TCG AGT TTA TGC CCC TAC TTT TGC TGC-3′). Each oligonucleotide primer was synthesized with HindIII (forward) or XhoI (reverse) restriction sites (underlined). The resulting PCR amplification products were cloned into pET28a digested with the same enzymes.

2.2. Generation of recombinant plasmids containing the P. vivax msp-3β gene

The nucleotide sequences corresponding to the N and C-terminal regions of *P. vivax* MSP-3β were obtained from the plasmids pGEX-1λT/FP-1(aa 35–375) or pGEX-2T/FP-2 (aa 385–654), respectively [10]. Both inserts were removed by enzymatic restriction with the enzyme EcoRI. The inserts were purified and cloned into the vector pHISa (FP-1) or pHISb (FP-2) digested with this same enzyme. After transformation in competent *E. coli* DH5α, the colonies that contained the different fragments of the *msp-3β* gene were selected by restriction analysis.

The nucleotide sequence corresponding to the full-length of *P. vivax* MSP-3β (aa 35–654) were obtained by PCR amplification from the plasmid pGEX-1λT (FP-3) [10]. The sense (5′-ATG GAT CCG AAC TTG AGA AAC GGA TGG TCA-3′) and anti-sense (5′-CGG ATC CTC TGC GAG TGT TTT ATG CGC TTC-3′) oligonucleotides contained the restriction site for the enzyme BamHI (underlined). The PCR product was separated on agarose gel and the 1.8 kb band was removed using the Geneclean kit (BIO101). DNA was cloned into the commercial vector pMOS-Blue (Amersham Biosciences) following the manufacturer's instructions. The sequence encoding *msp-3β* was confirmed by DNA sequencing. The *msp-3β* gene was removed from the pMOS vector by digestion with BamHI and cloned into the vector pET14b (Novagen) digested with this same enzyme. After transformation in competent *E. coli* DH5α, the colonies that contained the *msp-3β* gene were selected by restriction analysis.

The recombinant proteins based on MSP-3 sequences that we used in the present study are presented in Fig. 1.

2.3. Expression and purification of E. coli recombinant proteins MSP-3α and MSP-3β

E. coli BL21-DE3 (Novagen) containing the recombinant plasmids pHISa-MSP-3α (FP-1), pET28a-MSP-3α (CC4-5), pET28a-MSP-3α (CC4), pET28a-MSP-3α (CC5), pHISa-MSP-3β (FP-1), pHISb-MSP-3β (FP-2) and pET14b-MSP-3β (FP-3) were cultivated in 1 L of LB-ampicillin (100 μg/ml) at 37 °C shaken until they reached an OD_{600} of 0.6–0.8. Recombinant protein synthesis was induced by the presence of 0.01 to 1 mM isopropyl-β-D thiogalactopyranoside (IPTG, Invitrogen, Auckland, New Zealand) according dose response curve defined to each one recombinant. After 3 h, bacteria were pelleted by centrifugation and resuspended in sonication buffer (20 mM Tris–HCl pH 8.0, 200 mM NaCl, 1 mg/ml lysozyme and 1 mM phenylmethylsulfonyl fluoride (PMSF, Invitrogen). The bacteria were lysed on ice with the aid of a sonicator (Branson model 450, Danbury, CT). We applied 3 sonication cycles consisting of 5 min pulses at 5 min intervals. The bacterial lysate was centrifuged at 24,000 *g* for 60 min at 4 °C. The supernatant of the bacterial lysates was loaded onto pre-equilibrated Ni^{2+} Sepharose High Performance (Amersham Biosciences) or TALON Metal Affinity resins (BD Biosciences Clontech, Palo Alto, USA) and extensively washed with the wash buffer (20 mM Tris–HCl pH 8.0, 200 mM NaCl, pH 7.0, and 10% glycerin). Bound proteins were eluted with a wash buffer containing 0.3 M imidazole (USB) and the eluted material was dialyzed against 20 mM Tris–HCl, pH 8.0. After centrifugation at 18,000 *g* for 30 min at 4 °C and filtration through a 0.22 μm membrane, recombinant proteins were purified by ion-exchange chromatography using a Mono Q column (Amersham Biosciences) equilibrated with 20 mM Tris–HCl, pH 8.0, coupled to an FPLC system (Amersham Biosciences). The proteins were eluted with a linear 0 to 1 M NaCl gradient in Tris–HCl buffer. Fractions were analyzed by SDS-PAGE and stained with Coomassie blue. Fractions containing the recombinant proteins with a high degree of purity were pooled and extensively dialyzed against PBS. The protein concentration was determined spectrophotometrically at 280 nm using the Beer-Lambert Law: $Absorb(Prot) = \varepsilon \times l \times C$, where ε is the extinction coefficient, l is the path length in cm, and C is protein concentration (M). The extinction coefficient values were calculated by ProtParam tool [27]. Because

MSP-3α (CC4) protein lacks tryptophan or tyrosine in its sequence, the protein concentration was estimated by SDS-PAGE using Bovine Serum Albumin (Sigma) as the standard.

2.4. Spectroscopy

Circular dichroism measurements were made on a JASCO-J810 spectropolarimeter equipped with a temperature control system in a continuous mode. Recombinant MSP-3α (FP-1, CC4-5, CC4 and CC5) and MSP-3β (FP-1, FP-2 and FP-3) were diluted to 1.4–35 μM in PBS and loaded into a 1 or 5-mm quartz cuvette. Far-UV measurements (an average of ten scans) were carried out over wavelengths 260–200 nm with 1 nm bandwidth, 1 s response time, and 100 nm/min scan speed at 20 °C. Spectra were corrected by subtraction of the buffer signal. Molecular ellipticity, $[\theta]_{MRW}$, was calculated [28] and the secondary structure was estimated by computer analysis using CDNN software [29].

Emission fluorescence spectra of recombinant protein MSP-3α CC5 was recorded on an Aminco Bowman® Series 2 (SLM-AMINCO) fluorimeter. Emission fluorescence spectra of the protein at 1 mg/ml concentration in 20 mM Tris–HCl (pH 8.0) was obtained with excitation at 280 nm and with emission from 300 to 400 nm. The spectrum of MSP-3α CC5 was also obtained for the unfolded protein in 20 mM Tris–HCl, 6.2 M guanidinium choride buffer (pH 8.0).

2.5. Mass spectrometry

The monomeric mass of the two smaller fragments of the MSP-3α (CC4 and CC5) was verified using matrix-assisted laser desorption-ionization with time-of-flight mass spectrometry (MALDI-TOF MS). Acquisition of espectra was performed using an Ettan MALDI-ToF Pro mass spectrometer (GE healthcare) using Sinapinic acid matrix (SIN).

2.6. Size exclusion chromatography

The recombinants MSP3-α CC4 and CC5 in PBS, pH 7.4, were loaded onto a Superdex™ prep grade 200 XK 16/70 size exclusion column, with a flow rate of 0.5 ml/min The molecular mass and Stokes Radius (*Rs*) of the proteins in the different peak fractions were calculated by using a standard of globular proteins that were chromatographed under identical conditions based on [30]. Samples of all peak fractions were analyzed by SDS-PAGE for their protein composition.

2.7. Dynamic light scattering measurements

Dynamic light scattering (DLS) experiments were performed on a DynaPro-MS800 instrument (Protein Solutions Inc.) that monitors the scattered light at 90°, equipped with a temperature controlled microsampler. Recombinant proteins MSP3-α CC4 and CC5 at 1 mg/mL in Tris–HCl 20 mM (pH 8.0) were previously centrifuged at 13,000 g for 30 min at 4 °C and filtered (0.22 μm) to avoid unspecific large particles. Diffusion coefficients (*D*) were measured by monitoring intensity of scattered laser light at 20 °C. At least 100 independent measurements of 10 s each were collected. Only scattering peaks from 0.1 to 100.0 nm radius were used for calculation.

2.8. Analytical ultracentrifugation

Analytical ultracentrifugation (AUC) sedimentation equilibrium experiments were done with a Beckman Optima XL-A analytical ultracentrifuge as previously described [31]. MSP-3α CC5 was tested at concentrations from 0.25 to 1 mg/ml in Tris–HCl 20 mM and NaCl 100 mM pH 8.0, with speeds of 7000 to 11,000 (AN-60Ti rotor), and scan data acquisition at 280 nm. Analysis of the data involved the fitting of a model of absorbance versus cell radius data using nonlinear regression. All fittings were performed using the Origin software package (Microcal) supplied with the instrument. The Self-Association method was used to analyze the sedimentation equilibrium experiments using several models of association to fit the data. The distribution of the protein throughout the cell, obtained in the equilibrium sedimentation experiments, was fitted with the following equation [32]:

$$C = C_0 \exp\left[\frac{M(1 - Vbar\rho)\omega^2(r^2 - r_0)}{2RT}\right] \quad (1)$$

where *C* is the protein concentration at radial position *r*, C_0 is the protein concentration at radial position r_0, *M* is the molecular mass, *Vbar* is the partial specific volume, ω is the centrifugal angular velocity, *R* is the gas constant and *T* is the absolute temperature. The Sednterp software (www.jphilo.mailway.com/download.htm) was used to estimate the partial specific volume at 20 °C (0.7224 ml/g), the buffer density and the buffer viscosity.

3. Results

3.1. Expression and purification of recombinant proteins corresponding to the MSP-3α and MSP-3β of P. vivax

Four recombinant proteins representing the C-terminal region of MSP-3α (FP-1, CC4-5, CC4, and CC5) were used in this study. Three of these recombinant proteins correspond to fragments that are predicted to form coiled-coil (CC) tertiary structures. Attempts to generate recombinant proteins representing the full-length protein were unsuccessful because this protein was always cleaved at the N-terminus generating a shorter recombinant protein (data not shown). We used three recombinant proteins representing almost the full-length protein (FP-3), the N- (FP-1) or the C-terminal (FP-2) regions of the MSP-3β. All recombinant proteins expressed well in *E. coli* and were soluble in aqueous buffer in the absence of detergents. We observed that each protein migrated as single bands with few degradation products, and with apparent molecular weights of ~87 kDa (MSP-3α, FP-1), ~32 kDa (MSP-3α, CC4-5), ~13 kDa (MSP-3α, CC4), ~27 kDa (MSP-3α, CC5), ~60 kDa (MSP-3β, FP-1), ~57 kDa (MSP-3β, FP-2), and ~104 kDa (MSP-3β, FP-3) (Fig. 2). The proteins MSP-3α (CC4, CC5) and MSP-3β (FP-1, FP-2) appeared as a single band, while some degradation products were detectable to MSP-3α (FP-1, CC4-5) and MSP-3β (FP-3).

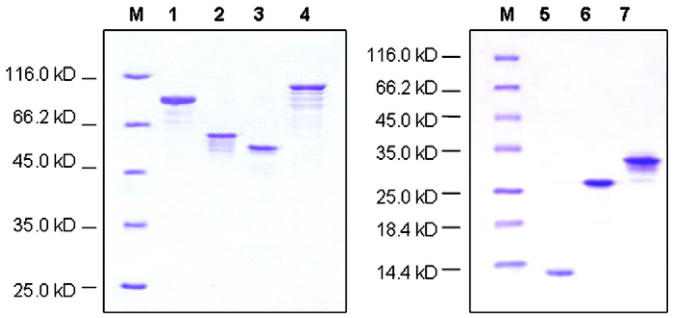

Fig. 2. SDS-PAGE analysis of the purified recombinant proteins corresponding to the MSP-3α and MSP-3β of *P. vivax*. Bacterial recombinant proteins were expressed and purified as described in Material and Methods section. M: molecular mass markers; 1: MSP-3α (FP-1); 2: MSP-3β (FP-1); 3: MSP-3β (FP-2); 4: MSP-3β (FP-3). 5: MSP-3α (CC4); 6: MSP-3α (CC5); 7 MSP-3α (CC4-5). Each lane was loaded with approximately 1.5 to 3.0 μg of recombinant protein.

3.2. Spectroscopy measurements of the recombinant MSP-3

To investigate the type of secondary structure present in each recombinant MSP-3, we examined them by far-UV CD spectroscopy (Fig. 3). The CD data were deconvoluted using the CDNN program, and the percentages of α-helix, other structures (anti-parallel, parallel and β-turn), and random coil were estimated. The CD spectrum for the seven recombinant proteins shows the two minima around 208 and 222 nm that are characteristic of α-helices, except MSP-3α (CC4) and MSP-3β (FP-2), which presented one minimum characteristic of random coil. The deconvoluted CD spectrum for the recombinant proteins predicted approximately the following percentages: C-terminal of MSP-3α (FP-1) 33% α-helix, 34% other structures, and 31% random coil; MSP-3α (CC4-5) 76% α-helix, 15% other structures, and 9% random coil; MSP-3α (CC4) 16% α-helix, 54% other structures, and 46% random coil; MSP-3α (CC5) 59% α-helix, 21% other structures, and 15% random coil (Fig. 3A). Notably, there is a relevant discrepancy between the numerical analysis and visual appearance of the CD spectrum to MSP-3α (CC4-5). The presence of degradation products detected in SDS-PAGE (Fig. 2), which may interfere in the biophysics measurements, may explain these results. The MSP-3α (CC5) CD spectra are consistent with the emission fluorescence spectra which suggested a folded protein (Fig. 4).

The CD spectrum of the MSP-3β (FP-1) protein predicts approximately 25% α-helix, 46% other structures, and 36% random coil. As such, the MSP-3 beta (FP-2) shows 16% α-helix, 53% other structures, and 44% random coil. The spectrum of full-length MSP-3β (FP-3) exhibits a strong α-helical signature and is estimated to be 48% helical, 25% other structures, and 22% random coil (Fig. 3B). The sum of the secondary structural elements calculated from the CD spectrum totals 95% to 116% showing confidence in the measurement and deconvolution.

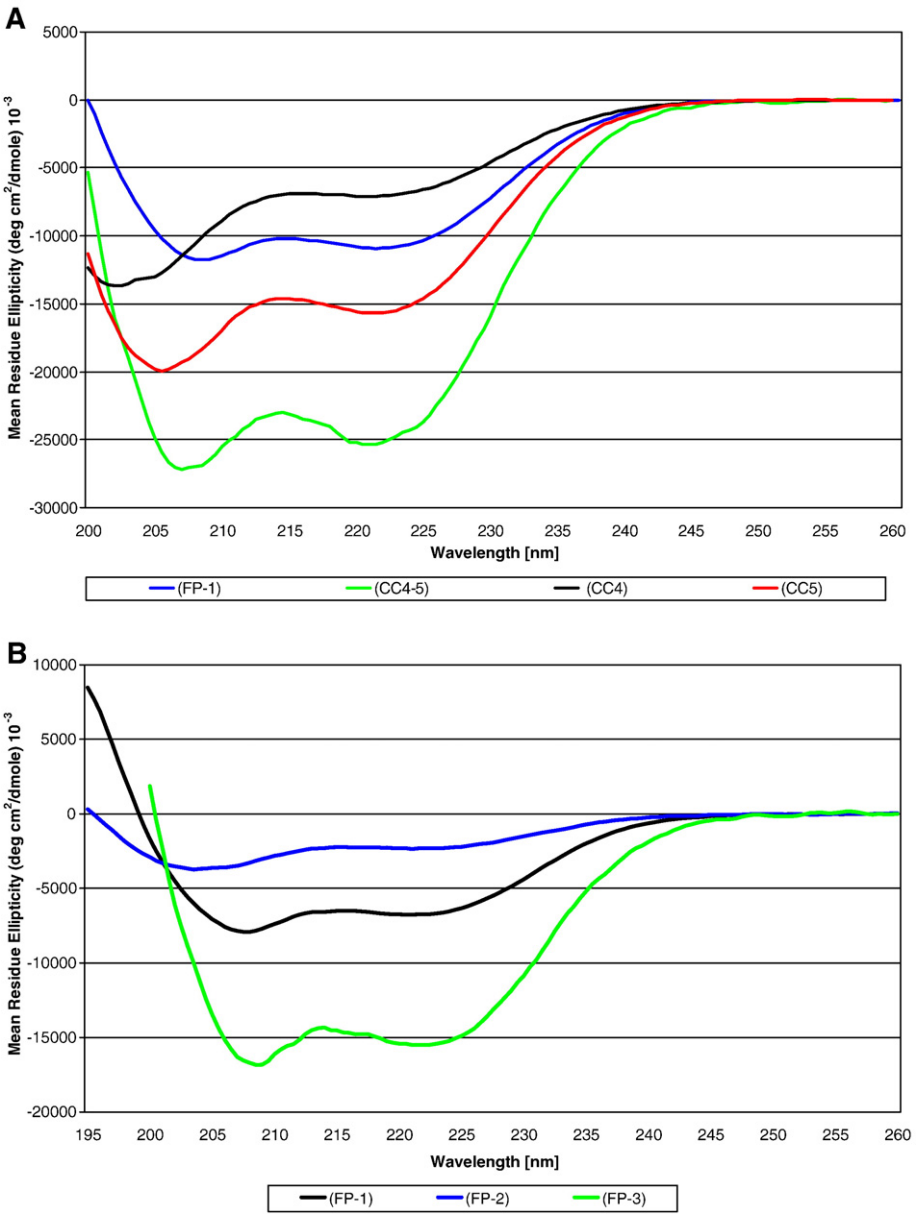

Fig. 3. CD spectra of the recombinants proteins corresponding to the MSP-3α and MSP-3β of *P. vivax*. A. CD spectra of MSP-3α (FP-1, CC4-5, CC4, and CC5) recorded from 200 to 260 nm. B. CD spectra of MSP-3β (FP-1, FP-2, and FP-3) recorded from 195 to 260 nm. The plot represents mean residue ellipticity (*m.r.e.*) of each recombinant protein.

3.3. Characterization of MSP3-α fragments by mass spectrometry analysis, size exclusion chromatography and dynamic light scattering

To investigate possible interaction between the regions that are predicted to form coiled-coil (CC) tertiary structures, we produced three shorter recombinant proteins containing subsets of the predicted domains of the C-terminal region of MSP3-α (Fig. 1). First, we submitted the proteins CC4 and CC5 to mass spectrometry (MS) analysis. The monomer mass assigned for the two recombinant proteins corresponded exactly to those predicted from the primary sequence (10176 kDa and 19427 kDa, respectively). During size exclusion chromatography, the proteins eluted at volumes corresponding to molecular weights that were larger than their monomeric masses. The CC4 eluted in two peaks with a Stokes radius of 30 and 20 Å and apparent molecular masses of 40 and 20 kDa, respectively. These data suggested that this MSP-3α fragment may be oligomers and the presence of these two peaks may represent different oligomeric states of the protein. In the case of CC5, after two-step chromatography to avoid artifact and unstable protein species, a single

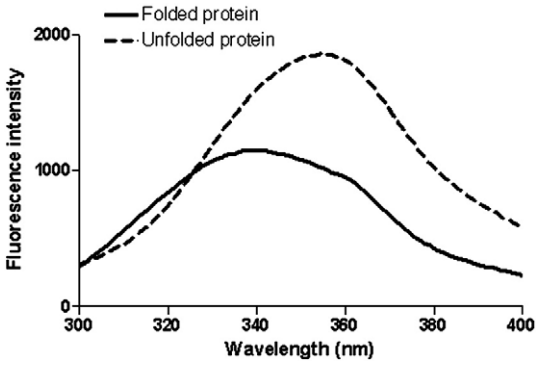

Fig. 4. Fluorescence. Recombinant protein MSP-3α CC5 fluorescence emission spectra at 20 °C measured with excitation at 280 nm and emission from 300 to 400 nm in 20 mM Tris-HCl (pH 8.0) buffer (solid line). The spectrum was also obtained for the recombinant protein in 20 mM Tris-HCl, 6.2 M guanidinium choride buffer (pH 8.0), i.e. the protein was unfolded (dashed line).

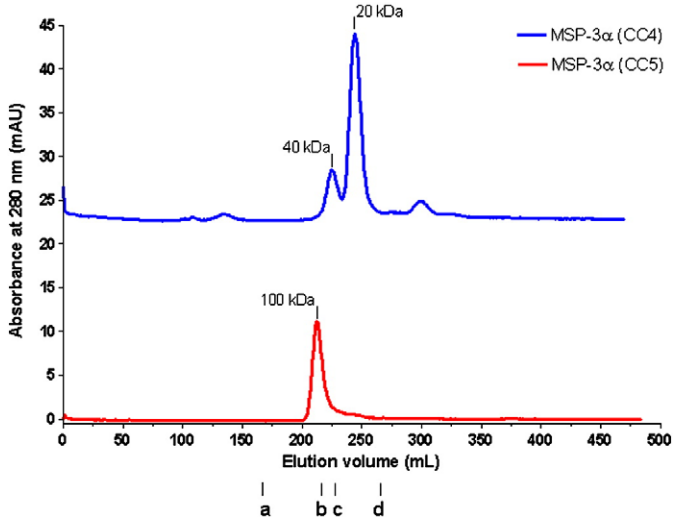

Fig. 5. Size exclusion chromatography of the MSP-3α coiled-coil regions. MSP-3α CC4 and CC5 were analyzed on Superdex 200 column. Elution volumes (*Ve*) of standard proteins: (a) Ferritin MW = 440 kDa, Rs = 5.79 nm, Ve = 160 ml; (b) Albumin MW = 67 kDa, Rs = 3.55 nm, Ve = 210 ml; (c) Ovalbumin MW = 43 kDa, Rs = 3.05 nm, Ve = 223 ml and (d) Ribonuclease A MW = 13.7 kDa, Rs = 1.64 nm, Ve = 262 ml are indicated by vertical lines.

peak with a Stokes radius of 38 Å and apparent molecular mass in the range of 92 to 100 kDa appeared (Fig. 5). Interestingly, the dynamic light scattering (DLS) experiments performed with each fragment (CC4 or CC5) showed that these proteins represent single species (Fig. 6).

3.4. Characterization of MSP3-α fragment (CC5) by analytical ultracentrifugation

To further investigate the oligomeric state and overall shape of MSP-3α, analytical ultracentrifugation was performed with the protein CC5. The equilibrium sedimentation profiles of CC5 were fitted to a tetrameric species at all concentrations and velocities tested (Fig. 7). This result indicated a molecular mass of 78.5 kDa from which the radius of a hypothetical rigid sphere with an identical volume as the molecule of interest (R_{hyp}) was predicted using the following equation:

$$R_{hyp} = (3M\ Vbar/4\pi N)^{1/3} \quad (2)$$

where M is the molecular mass, and N is the Avogadro's number. The actual hydrodynamic radius (R_H) was calculated from the size

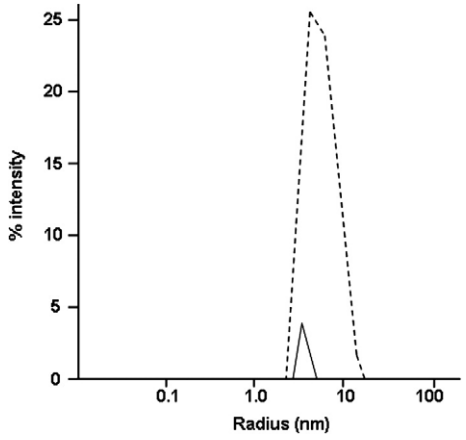

Fig. 6. Recombinant proteins MSP-3α CC4 and CC5 Dynamic Light Scattering measurements. The figure shows single dispersivity of both recombinant proteins MSP-3α CC4 (solid line) and MSP-3α CC5 (dashed line) by the intensity of scattered laser light correlated to the estimated Stokes radium calculation using peaks from 0.1 to 100.0 nm radius.

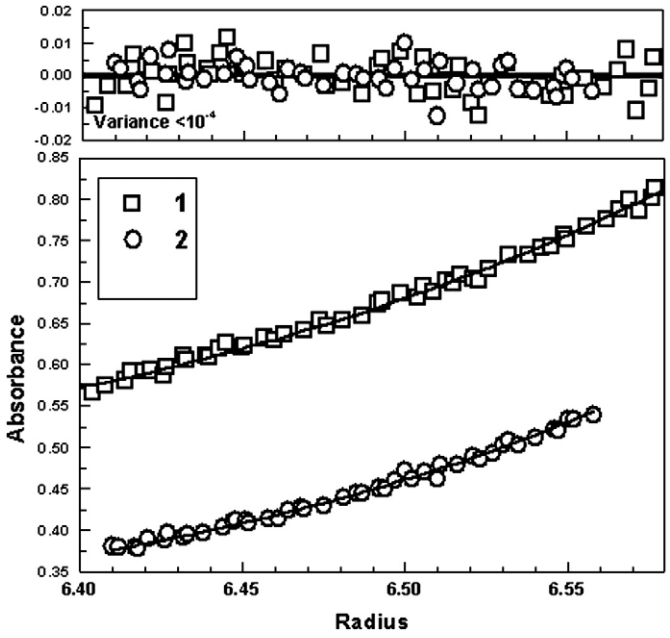

Fig. 7. Analytical ultracentrifugation of MSP-3α (CC5). The sedimentation equilibrium analyses were performed from 0.25–1 mg/ml in 20 mM Tris–HCl pH 8, and 100 mM NaCl, at 10 °C, with speeds of 7000, 8000, and 9000 rpm (AN-60Ti rotor), and scan data acquisition at 280 nm. The best fit was determined by the randomness of the distribution of the residuals and by minimization of the variation of the variance. The figure shows protein sedimentation equilibrium profiles at 0.5 mg/ml at 9000 rpm (1) and 8000 rpm (2). The data fit well to tetrameric species (see the residuals plot in the top panel).

exclusion chromatograph and used to calculate the frictional coefficient (f) via Stokes equation, where η is the viscosity of the solvent [33]:

$$f = 6\pi\ \eta\ R_H \quad (3)$$

Similarly, the predicted frictional coefficient for a rigid sphere with an identical volume as the molecule of interest (f_o) was calculated from R_{hyp}. From those results, we calculated the so-called Perrin or shape factor F, which represents a ratio of the measured frictional coefficient f to the frictional coefficient f_0 and is informative of the shape of the molecule [34]. In this way, the Perrin factor provides information about the shape of the particle because the further away it is from 1, the less spherical (globular) the shape is. Our analysis revealed a Perrin shape factor of 1.35, indicating that the protein is not globular. From this two explanations can be drawn, one, that this domain is unfolded but such hypothesis is ruled out by circular dichroism analysis (Fig. 3A) and emission fluorescence spectra (Fig. 4), which indicated a well-folded protein, and the other, that the domain is elongated, which is well in agreement with these domains forming a coil-coiled structure.

4. Discussion

MSP-3α and MSP-3β are associated with the merozoite surface of *P. vivax* [9] and [10]. Both proteins, like PfMSP-3 have neither a classical hydrophobic transmembrane domain nor a consensus sequence for post-translational modification with GPI. As reported for PfMSP-3, the central core domain of each of the *P. vivax* homologues is predicted to form α-helical secondary structure and coiled-coil tertiary structures. In order to make an initial characterization of the structure of PvMSP-3α and PvMSP-3β, we have generated in *E. coli* seven recombinant proteins, four representing the C-terminal region of MSP-3α and three representing different regions of MSP-3β (N- and C-terminal and almost full-length protein). Initially, we performed CD experiments with different MSP-3 recombinants. Our results indicate that: i) the proteins CC5 (MSP-3α) and

FP-3 (MSP-3β) are well-folded; ii) some proteins, such as FP-1 and CC4-5 (MSP-3α), and FP-1 (MSP-3β), presented a partially folded intermediate conformation, and iii) the proteins CC4 (MSP-3α) and FP-2 (MSP-3β) appeared only to be partially structured. The significant percentage of a -helix estimated from the CD experiments performed on recombinant protein representing almost the full-length protein of MSP-3β (FP-3) is consistent with many characteristics of full-length of PfMSP-3 [22].

Coiled coils are protein interaction motifs that consist of left-handed supercoiled assemblies of two or more α-helices. These protein structures are commonly involved in forming both intra- and inter-molecular binding interactions. It has been hypothesized that these proteins interact through the central alanine-rich and terminal glutamic acid-rich domains with other proteins or positively charged moieties on the surface of the merozoite, generating the structural complexity of the coat that has been observed by electron microscopy [35]. To explore possible interactions involving predicted coiled-coil domains of MSP-3α, we performed biophysical studies with the fragment CC5. As observed for the full length of PfMSP-3 [22], we found by size exclusion chromatography that CC5 forms oligomers in solution. Most relevant was the fact that analytical ultracentrifugation experiments indicated that CC5 is a non-globular protein and probably exists as an elongated tetrameric species. However, the leucine zipper-like regions, which are absent in MSP-3 of *P. vivax* [9] and [10], are not required for oligomer formation as observed for PfMSP-3 [22].

In parallel, we also performed initial crystallization trials for the different proteins. Various crystals were obtained and one of them (MSP-3α, FP-1) diffracted X-rays only poorly (10 Å resolution). Unfortunately, after refinement of the crystallization conditions, crystal improvement was insufficient, leading to a maximum diffraction resolution of 3.87 Å [36]. Determining the three-dimensional structure of *Plasmodium* proteins has been particularly complicated for many reasons, including proteins that contain large non-globular domains [37].

To sum up, this study represents the first description of the biophysical characteristics of the *P. vivax* MSP-3 α and β proteins expressed and purified from *E. coli*. The data generated indicate that recombinant proteins based on predicted coiled-coil domains of MSP-3α form oligomeric and elongated molecules consistent with previous data relating to PfMSP-3 [22].

Acknowledgments

We are particularly grateful to Vanessa C. Tavares, Cristiane R. Guzzo, and Fabio Schaberle for their technical assistance. This work was supported by FAPESP grants 01/07535-0 (SMolBNet) and 01/08498-0 (regular), and The Millennium Institute for Vaccine Development and Technology (CNPq - 420067/2005-1). MCSJ is supported by fellowships from FAPESP. CHIR, JARGB, MMR and ISS are supported by fellowships from CNPq.

References

[1] K. Mendis, B.J. Sina, P. Marchesini, R. Carter, The neglected burden of *Plasmodium vivax* malaria, Am. J. Trop. Med. Hyg. 64 (2001) 97–106.
[2] J.K. Baird, Neglect of *Plasmodium vivax* malaria, Trends Parasitol. 23 (2007) 533–539.
[3] S. Herrera, G. Corradin, M. Arevalo-Herrera, An update on the search for a *Plasmodium vivax* vaccine, Trends Parasitol. 23 (2006) 122–128.
[4] S.P. Wertheimer, J.W. Barnwell, *Plasmodium vivax* interaction with the human Duffy blood group glycoprotein: identification of a parasite receptor-like protein, Exp. Parasitol. 69 (1989) 340–350.
[5] X.D. Fang, D.C. Kaslow, J.H. Adams, L.H. Miller, Cloning of the *Plasmodium vivax* duffy receptor, Mol. Biochem. Parasitol. 44 (1991) 125–132.
[6] H.A. del Portillo, S. Longacre, E. Khouri, P. David, Primary structure of the merozoite surface antigen 1 of *Plasmodium vivax* reveals sequences conserved between different *Plasmodium* species, Proc. Natl. Acad. Sci. U. S. A. 88 (1991) 4030–4034.
[7] M.R. Galinski, C.C. Medina, P. Ingravallo, J.W. Barnwell, A reticulocyte-binding protein complex of *Plasmodium vivax* merozoites, Cell 69 (1992) 1213–1226.
[8] Q. Cheng, A. Saul, Sequence analysis of the apical membrane antigen 1 (AMA-1) of *Plasmodium vivax*, Mol. Biochem. Parasitol. 65 (1994) 183–187.
[9] M.R. Galinski, C. Corredor-Medina, M. Povoa, J. Crosby, P. Ingravallo, J.W. Barnwell, *Plasmodium vivax* merozoite surface protein-3 contains coiled-coil motifs in an alanine-rich central domain, Mol. Biochem. Parasitol. 101 (1999) 131–147.
[10] M.R. Galinski, P. Ingravallo, C. Corredor-Medina, B. Al-Khedery, M. Povoa, J.W. Barnwell, *Plasmodium vivax* merozoite surface proteins-3β and-3γ share structural similarities with *P. vivax* merozoite surface protein-3α and define a new gene family, Mol. Biochem. Parasitol. 115 (2001) 41–53.
[11] E. Vargas-Serrato, J.W. Barnwell, P. Ingravallo, F.B. Perler, M.R. Galinski, Merozoite surface protein-9 of *Plasmodium vivax* and related simian malaria parasites is orthologous to p101/ABRA of *P. falciparum*, Mol. Biochem. Parasitol. 120 (2002) 41–52.
[12] J.C. Rayner, V. Corredor, D. Feldman, P. Ingravallo, F. Iderabdullah, M.R. Galinski, J.W. Barnwell, Extensive polymorphism in the *Plasmodium vivax* merozoite surface coat protein MSP-3α is limited to specific domains, Parasitology 125 (2002) 393–405.
[13] M.C. Bruce, M.R. Galinski, J.W. Barnwell, G. Snounou, K.P. Day, Polymorphism at the merozoite surface protein-3α locus of *Plasmodium vivax*: global and local diversity, Am. J. Trop. Med. Hyg. 61 (1999) 518–525.
[14] M.C. Bruce, C.A. Donnelly, M.P. Alpers, M.R. Galinski, J.W. Barnwell, D. Walliker, K.P. Day, Cross-species interactions between malaria parasites in humans, Science 287 (2000) 845–848.
[15] M.C. Bruce, J.W. Barnwell, C.A. Donnelly, M. Walmsley, M.P. Alpers, D. Walliker, K.P. Day, Genetic diversity and dynamics of *Plasmodium falciparum* and *Plasmodium vivax* populations in multiply infected children with asymptomatic malaria infections in Papua New Guinea, Parasitology 121 (2000) 257–272.
[16] I. Mueller, J. Kaiok, J.C. Reeder, A. Cortes, The population structure of *Plasmodium falciparum* and *Plasmodium vivax* during an epidemic of malaria in the Eastern Highlands of Papua New Guinea, Am. J. Trop. Med. Hyg. 67 (2002) 459–464.
[17] R. Ord, S. Polley, A. Tami, C.J. Sutherland, High sequence diversity and evidence of balancing selection in the Pvmsp3 alpha gene of *Plasmodium vivax* in the Venezuelan Amazon, Mol. Biochem. Parasitol. 144 (2005) 86–93.
[18] C.N. Mascorro, K. Zhao, B. Khuntirat, J. Sattabongkot, G. Yan, A.A. Escalante, L. Cui, Molecular evolution and intragenic recombinantion of the merozoite surface protein MSP-3 alpha from the malaria parasite *Plasmodium vivax* in Thailand, Parasitology 131 (2005) 25–35.
[19] L. Cui, C.N. Mascorro, Q. Fan, K.A. Rzomp, B. Khuntirat, G. Zhou, H. Chen, G. Yan, J. Sattabongkot, Genetic diversity and multiple infections of *Plasmodium vivax* malaria in western Thailand, Am. J. Trop. Med. Hyg. 68 (2003) 613–619.
[20] J.C. Rayner, C.S. Huber, D. Feldman, P. Ingravallo, M.R. Galinski, J.W. Barnwell, *Plasmodium vivax* merozoite surface protein PvMSP-3 beta is radically polymorphic through mutation and large insertions and deletions, Infect. Genet. Evol. 4 (2004) 309–319.
[21] G.A. Bentley, Functional and immunological insights from the three-dimensional structures of *Plasmodium* surface proteins, Curr. Opin. Microbiol. 9 (2006) 395–400.
[22] B.R. Burgess, P. Schuck, D.N. Garboczi, Dissection of merozoite surface protein 3, a representative of a family of *Plasmodium falciparum* surface proteins, reveals an oligomeric and highly elongated molecule, J. Biol. Chem. 280 (2005) 37236–37245.
[23] C.W. Kauth, U. Woehlbier, M. Kern, Z. Mekonnen, R. Lutz, N. Mucke, J. Langowski, H. Bujard, Interactions between merozoite surface proteins 1, 6, and 7 of the malaria parasite *Plasmodium falciparum*, J. Biol. Chem. 42 (2006) 31517–31527.
[24] C. Trucco, D. Fernandez-Reyes, S. Howell, W.H. Stafford, T.J. Scott-Finnigan, M. Grainger, S.A. Ogun, W.R. Taylor, A.A. Holder, The merozoite surface protein 6 gene codes for a 36 kDa protein associated with the *Plasmodium falciparum* merozoite surface protein-1 complex, Mol. Biochem. Parasitol. 112 (2001) 91–101.
[25] M.J. Blackman, H.G. Heidrich, S. Donachie, J.S. McBridge, A.A. Holder, A single fragment of a malaria merozoite surface protein remains on the parasite during red blood cell invasion and is the target of invasion-inhibiting antibodies, J. Exp. Med. 172 (1990) 379–382.
[26] P. Sheffield, S. Garrard, Z. Derewenda, Overcoming expression and purification problems of RhoGDI using a family of "Parallel" expression vectors, Prot. Exp. Purif. 15 (1999) 34–39.
[27] E. Gasteiger, C. Hoogland, A. Gattiker, S. Duvaud, M.R. Wilkins, R.D. Appel, A. Bairoch, in: J.M. Walker (Ed.), The Proteomics Protocols Handbook, Humana Press, Hatfield, 2005, pp. 571–608.
[28] C.H.I. Ramos, A spectroscopic-based laboratory experiment for protein conformational studies, Biochem. Mol. Biol. Educ. 32 (2004) 31–34.
[29] G. Bohm, R. Muhr, R. Jaenicke, Quantitative analysis of protein far UV circular dichroism spectra by neural networks, Protein Eng. 5 (1992) 191–195.
[30] J.I. Hwang, R. Schlesinger, C.W. Koch, Irregular dimerization of guanylate cyclase-activating protein 1 mutants causes loss of target activation, Eur. J. Biochem. 271 (2004) 3785–3793.
[31] W.C.B. Regis, J. Fattori, M.M. Santoro, M. Jamin, C.H.I. Ramos, On the difference in stability between horse and sperm whale myoglobins, Arch. Biochem. Biophys. 436 (2005) 168–177.
[32] M.L. Johnson, J.J. Correia, D.A. Yphantis, H.R. Halvorson, Analysis of data from the analytical ultracentrifuge by nonlinear least-squares techniques, Biophys. J. 36 (1981) 575–588.
[33] D.C. Teller, E. Swanson, C. DeHaen, The translation frictional coefficient of proteins, Methods Enzymol. 61 (1979) 103–124.
[34] C.R. Cantor, P.R. Schimmel, in: L.W. McCombs (Ed.), Biophysical chemistry, Part II: techniques for the study of biological structure and function, W.H. Freeman and Company, New York, 1980, pp. 539–590.
[35] M.R. Galinski, J.W. Barnwell, *Plasmodium vivax*: merozoites, invasion of reticulocytes and considerations for vaccine development, Parasitol. Today 12 (1996) 20–29.
[36] J.A. Barbosa, L.E. Nett, C.S. Farah, S. Schenkman, R. Meneghini, The structural molecular biology network of the State of Sao Paulo, Brazil, An. Acad. Bras. Cienc. 2 (2006) 241–253.
[37] D.J. Carucci, *Plasmodium* post-genomics: an update, Trends Parasitol. 20 (2004) 558–561.